Langmuir

Letter

pubs.acs.org/Langmuir

Modeling Negative Cooperativity in Streptavidin Adsorption onto Biotinylated Microtubules

Siheng He,[†] Amy T. Lam,[†] Yolaine Jeune-Smith,[†] and Henry Hess*

Department of Biomedical Engineering, Columbia University, New York, New York 10027, United States

Supporting Information

ABSTRACT: The nanoscale architecture of binding sites can result in complex binding kinetics. Here, the adsorption of streptavidin and neutravidin to biotinylated microtubules is found to exhibit negative cooperativity due to electrostatic interactions and steric hindrance. This behavior is modeled by a newly developed kinetic analogue of the Fowler−Guggenheim adsorption model. The complex adsorption kinetics of streptavidin to biotinylated structures needs to be considered when these intermolecular bonds are employed in self-assembly and nanobiotechnology.

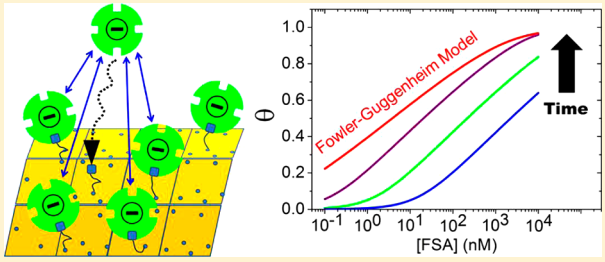

INTRODUCTION

Biotin−streptavidin linkages are a key tool in supramolecular chemistry and nanobiotechnology because of their low dissociation rate and their ability to connect molecular and nanoscale building blocks with high specificity.[1−5] For example, by binding streptavidin molecules to biotinylated microtubules, it is possible to tune the assembly of microtubules into larger structures,[6−11] capture biotinylated analytes such as antibodies and DNA,[12−14] and create defined obstacles that hinder kinesin motor movement along the microtubule.[15] In all of these cases, it is essential that the streptavidin coverage on the microtubule be well-controlled. Although initial experiments hinted that streptavidin adsorption could be predicted by the Langmuir model,[13] it was later shown that coverage had not yet reached saturation,[15] suggesting that the adsorption behavior is more complex. To control the degree of streptavidin coverage, the adsorption behavior needs to be clearly understood.

Because of the high density of binding sites on the microtubule and the negative charge of the streptavidin molecules, negative cooperativity between binding sites is one possible explanation for the complex adsorption behavior. Although cooperativity cannot be taken into account with the Langmuir model,[16] extensions such as the Temkin model and the Fowler−Guggenheim model account for interactions between adsorbate molecules under equilibrium conditions.[17−19] However, under typical experimental conditions,[1−15] equilibrium is not reached because the repulsive interactions between adsorbates dramatically slow the adsorption process.

The two major kinetic adsorption models are the Langmuir-type kinetic adsorption model and the random sequential adsorption (RSA) model. The former is the kinetic analog to the Langmuir equilibrium model (i.e., it assumes identical and independent binding sites) and is therefore unsuitable for this system.[20] The RSA model also cannot be used because it only takes into account steric interactions between adsorbate molecules and neglects any cooperative effects on the binding probability of accessible binding sites.[21]

Here, we develop and test a kinetic adsorption model using the adsorption of streptavidin onto biotinylated microtubules as an example of a system where interacting particles adsorb to densely situated, identical binding sites. At steady state, our kinetic model reduces to the Fowler−Guggenheim equilibrium model. By fitting the model to experimental data, we obtain values for the intrinsic activation energy and the average adsorbate interaction energy of the transition state.

RESULTS AND DISCUSSION

Microtubules are hollow tubes composed of 12−15 protofilaments,[22] which are long chains of alternating α- and β-tubulin (Figure 1a). Both tubulin subunits have diameters of approximately 4 nm and together form a tubulin heterodimer. Each of the tubulin dimers presents several lysine groups on its outer surface after its assembly into a microtubule. On average, one of these lysines is functionalized with biotin (according to the manufacturer) so that neighboring binding sites are spaced between 0.5 and 11 nm (SI). Biotin-XX (6-((6-((biotinoyl)-amino)hexanoyl)amino)hexanoic acid), the long-chain biotin derivative used here, has a long, flexible linker (1.7 nm).[23,24]

Fluorescently tagged streptavidin with a diameter of 4 nm binds to the biotin linkers on the surface of the microtubule (Figure 1b). Streptavidin has four binding sites that can form strong bonds to biotin ($K_d \approx 10^{-14}$ M).[25] The long biotin linker allows a bound streptavidin molecule to access its surroundings. Thus, neighboring adsorbate molecules are able

Received: May 18, 2012
Revised: July 2, 2012
Published: July 5, 2012

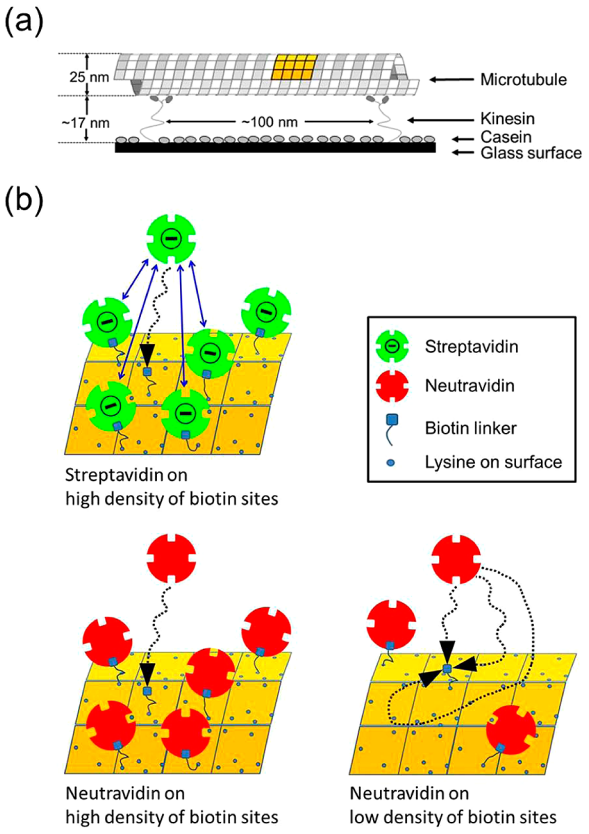

Figure 1. (a) Experimental system: biotinylated microtubules are tethered to a surface by kinesin motor proteins, and the adsorption of fluorescently labeled streptavidin or neutravidin is followed with fluorescence microscopy. (b) Electrostatic and steric interactions can be varied by replacing streptavidin with neutravidin and by changing the density of biotinylated tubulins.

to interact. The radius of interaction is further increased by streptavidin's negative charge.[26]

A range of streptavidin concentrations (0.1 nM, 1 nM, 10 nM, 100 nM, 1 μM, and 10 μM) are added to the system and incubated for 10 min, consistent with published protocols of similar experiments.[6,9,12,13,15,27] Excess streptavidin is flushed out of the system, leaving only bound adsorbate molecules behind. At this point in time, equilibrium has not been reached (SI). We then image the microtubules and measure the fluorescence intensity, which is proportional to the degree of coverage (Figure 2). Coverage is plotted as a function of streptavidin concentration (Figure 3a).

The fluorescence intensity increases over the whole range of concentrations tested rather than plateauing after a sharp increase over a narrow range of adsorbate concentrations, as expected from a Langmuirian adsorption process. Because the microtubules are long and are held about 20 nm above the surface by the widely separated kinesin tethers,[28] binding sites on the microtubule surface have identical local environments and binding strengths. Therefore, the gradual increase in coverage must originate from negative cooperativity due to interactions between adsorbate molecules.

To eliminate electrostatic interactions between adsorbate molecules, neutravidin (pI 6.3) can be used as an electrically neutral alternative to streptavidin (pI 5).[29] Neutravidin has approximately the same size and structure and also binds strongly to biotin ($K_d \approx 10^{-15}$ M).[25] The coverage increases

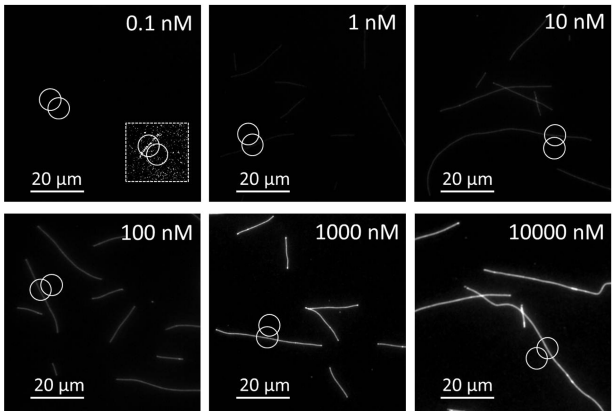

Figure 2. Fluorescence microscopy images of fluorescent streptavidin adsorbing for 10 min to biotinylated microtubules tethered to kinesin-coated surfaces. Individual intensity measurements are taken by summing the counts for a circle of 8 μm diameter centered on the microtubule and background corrected by subtracting the counts in an identically sized circle close to the microtubule. The inset in the first panel is a contrast-enhanced image of the measured microtubule.

more rapidly, bringing the adsorption curve closer to a Langmuirian fit (Figure 3b).

Steric interactions can be reduced by increasing the average distance between biotin sites by 60% via a 2.5-fold dilution of the biotinylated tubulin during the polymerization of the microtubule. Again, the range of concentrations over which coverage increases narrows, and the adsorption behavior becomes almost Langmuirian (Figure 3c). This implies that the observed adsorption behavior of streptavidin is due to a combination of electrostatic and steric interactions between adsorbate molecules.

Because of the absence of models of adsorption kinetics that account for interactions between adsorbates, we formulated a kinetic model that converges to the Fowler–Guggenheim model at steady state ($d\theta/dt = 0$). We assume that the change in coverage (θ) over time is determined by the rate of adsorption and the rate of desorption ($k_{off} = 5.4 \times 10^{-6}$ s^{-1}).[30] The adsorption rate is given by the product of the sticking probability (term I in eq 1) and the molecular flux to the

$$\frac{d\theta}{dt} = (1-\theta)\exp\left(-\frac{E_0+E_i\theta}{kT}\right) \times c\frac{N_A}{\sigma_{max}}\sqrt{\frac{RT}{2\pi M}} - k_{off}\theta \quad \text{(Eq. 1)}$$

I II

surface (term II in eq 1).[31] The sticking probability is dependent on the probability that an adsorbate molecule finds an open site and the probability that the adsorbing molecule has enough energy to overcome the apparent activation energy barrier. The energy barrier itself consists of two terms: the intrinsic activation energy of bond formation (E_0) and the additional energy needed to overcome the nearest-neighbor interactions at the transition state (E_i). Because the sticking probability is low ($\sim 10^{-6}$),[32] as is the case with other bonds in solution,[33] the surface acts as a nearly perfect reflector, and the adsorbate concentration can be assumed to be constant throughout the solution. It is therefore possible to use the Hertz–Knudsen equation to determine the molecular flux (term II), which depends on the concentration of the bulk

dx.doi.org/10.1021/la302034h | *Langmuir* 2012, 28, 10635–10639

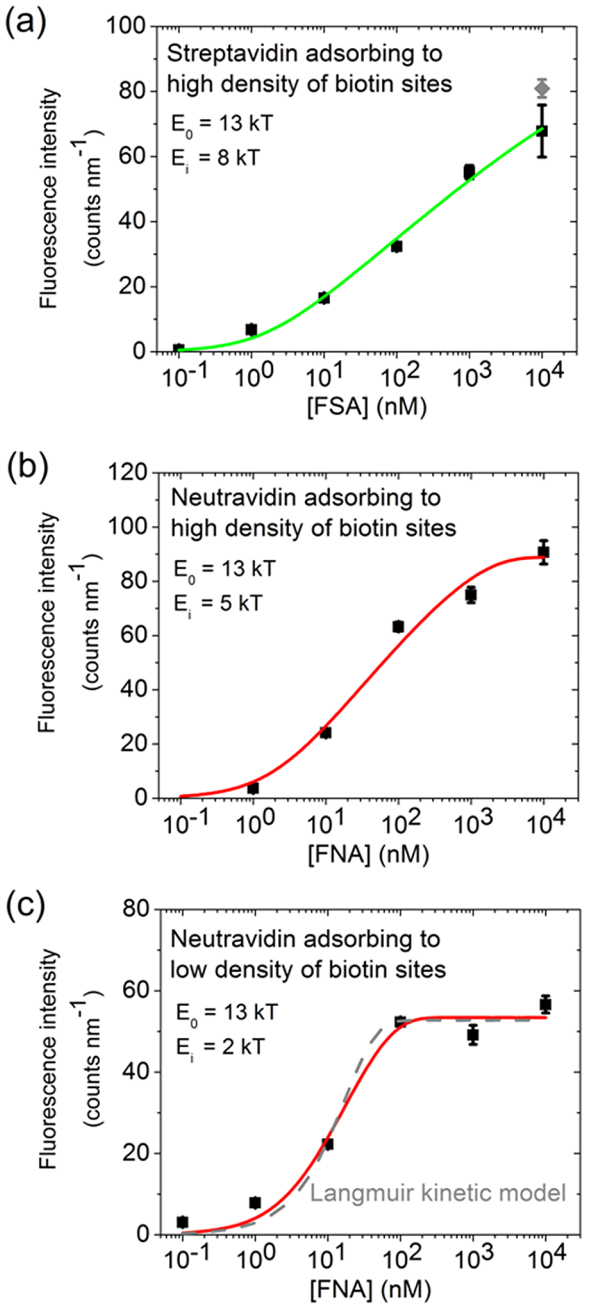

Figure 3. Experimental data and fits. (a) Adsorption of fluorescently tagged streptavidin (FSA) onto microtubules polymerized with 100% biotin tubulin. The gray data point corresponds to the maximum intensity (measured after 24 h of incubation). (b) Adsorption of fluorescently tagged, electrically neutral neutravidin (FNA) onto 100% biotin microtubules decreases the interaction energy by about $3kT$. (c) Adsorption of fluorescently tagged neutravidin onto 60% rhodamine/40% biotin microtubules increases the average distance between binding sites. Because of random fluctuations in lamp intensity, intensity measurements between experiments cannot be directly compared. Error bars represent the standard error of the mean of 24–30 individual intensity measurements.

solution c, the density of binding sites σ_{max}, the temperature T, and the molecular weight of the adsorbate molecule M.[34] Hence, the complete equation describing our system is eq 1.

We numerically integrated and fit eq 1 to the data, with E_0 and E_i being the fit parameters (Figure 3). For streptavidin adsorbing onto 100% biotinylated microtubules, we obtained values for the intrinsic activation energy of $(13 \pm 1)kT$ and the interaction energy of $(8 \pm 2)kT$. For comparison, the intrinsic activation energy of free biotin adsorption to streptavidin in PBS buffer has been measured to be $(10 \pm 4)kT$.[30,35] For neutravidin adsorbing onto 100% biotinylated microtubules, the interaction energy decreases to $(5 \pm 3)kT$ whereas the intrinsic binding energy stays the same ($(13 \pm 2)kT$), implying that the charge on streptavidin adds an additional $3kT$ to the activation energy barrier. When 40% biotin tubulin is used with neutravidin, the interaction energy further decreases to (2 ± 2) kT. The decreased binding site density reduces the steric hindrance, which accounts for the decreased activation energy. Thus, we conclude that steric hindrance contributes $5kT$ of activation energy to streptavidin binding to 100% biotinylated microtubules.[36] This can be accounted for by the geometry of the system (SI).

We also considered the possibility of multivalent binding of streptavidin. However, given the adsorption data, it is unlikely that this occurs to a large extent (SI). Control experiments with gliding microtubules in the presence of ATP reproduced the previously described decrease in gliding speed in proportion to the streptavidin coverage[15] but also showed that streptavidin adsorption was not affected by kinesin activity (SI).

CONCLUSIONS

Although adsorption curves of analyte detection systems are often fit to multiparameter expressions,[37,38] these curves do not provide mechanistic insight. Here, we develop a new kinetic adsorption model (Figure 4) and determine the intrinsic activation energy and the increase in activation energy due to interactions between binding sites. It is possible to apply this kinetic model to any adsorption process with identical binding sites and interacting adsorbate molecules (e.g., kinesin adsorption onto microtubules).[39,40]

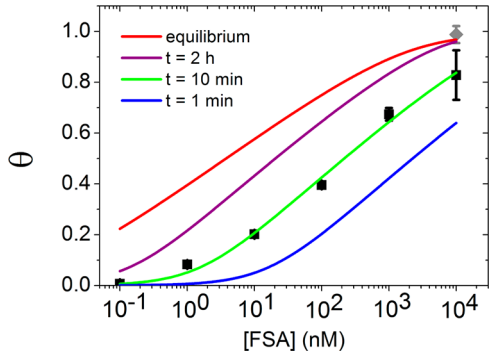

Figure 4. Theoretical prediction of streptavidin adsorption behavior for different incubation times. Curves are generated on the basis of the kinetic model, with parameters obtained from the model fit to data from streptavidin adsorption onto 100% biotinylated microtubules (E_0 = $13kT$ and E_i = $8kT$).

Previous studies of avidin adsorption onto biotinylated microtubules showed that protein interactions may influence the adsorption behavior at equilibrium.[41,42] On the basis of the adsorption data and theory, we verify that both electrostatic and steric interactions play a large role in determining the adsorption kinetics of streptavidin to biotinylated microtubules because of their contributions to the apparent activation energy. In general, systems that must be sensitive to a wide range of concentrations (e.g., chemical sensors) would benefit from

dx.doi.org/10.1021/la302034h | Langmuir 2012, 28, 10635–10639

having densely situated binding sites allowing for negatively cooperative interactions whereas less dense configurations would enhance the efficiency of adsorption.

MATERIALS AND METHODS

Microtubule Preparation. The 100% biotin microtubules were polymerized from a 20 μg aliquot of biotinylated bovine brain tubulin (T333P, lot 013, Cytoskeleton, Denver, CO) in 6 μL of BRB80 buffer consisting of 80 mM piperazine diethanesulfonic acid, 1 mM magnesium chloride ($MgCl_2$), and 1 mM ethylene glycol tetraacetic acid, pH 6.9, with potassium hydroxide (KOH) (if not specifically mentioned, all chemicals were purchased from Sigma, St. Louis, MO) and 4 mM $MgCl_2$, 1 mM guanosine triphosphate, and 5% dimethyl sulfoxide at 37 °C. After 30 min, the microtubules were stabilized and diluted 100-fold in BRB80 containing 10 μM paclitaxel. The 40% biotin microtubules were created by mixing rhodamine-labeled tubulin with biotinylated tubulin before microtubule assembly.

Kinesin Preparation. A kinesin construct consisting of the wild-type, full-length *Drosophila melanogaster* kinesin heavy chain and a C-terminal His-tag was expressed in *Escherichia coli* and purified using a Ni-NTA column.[43]

Fluorescent Streptavidin/Neutravidin Adsorption Assay. The experiments were performed in 75−100-μm-high, 1-cm-wide flow cells assembled with two glass coverslips (Fisher Scientific, Pittsburgh, PA) and held together by double-sided Scotch tape. A casein-containing solution (0.5 mg mL^{-1} in BRB80) was perfused into a flow cell and allowed to adsorb for 5 min. Next, 30 μL of kinesin solution was perfused into the flow cell and was allowed to adsorb for 5 min. Thereafter, 30 μL of microtubule solution diluted 10-fold in adenosine imidotriphosphate (AMP-PNP)-antifade solution (BRB80 with 1 mM AMP-PNP, 20 mM D-glucose, 20 μg mL^{-1} glucose oxidase, 8 μg mL^{-1} catalase, 10 mM dithiothreitol, and 0.2 mg mL^{-1} and 10 μM paclitaxel) was perfused into the flow cell and was allowed to adsorb for 5 min. AMP-PNP is a nonhydrolyzable analog of ATP that prevents microtubule gliding, allowing kinesin motors to hold microtubules in the absence of ATP.

Streptavidin/neutravidin was adsorbed to surface-immobilized microtubules by washing out unbound microtubules twice with 30 μL of AMP-antifade solution and flowing 30 μL of streptavidin/neutravidin solution (Alexa Fluor 488 conjugated streptavidin or Rhodamine Red-X conjugated neutravidin from Invitrogen, Carlsbad, CA) into the flow cell. Excess streptavidin/neutravidin was removed after 10 min of incubation by washing twice with 30 μL of AMP-PNP-antifade solution.

Image Acquisition and Data Analysis. The flow cells were imaged using a Nikon TE2000-U Epi-fluorescence microscope (Nikon, Melville, NY) equipped with an X-cite 120 lamp (EXFO, Ontario, Canada), an iXON DU885LC EMCCD camera (Andor, South Windsor, CT), and a 40× oil objective (NA 1.30). The exposure times were 5 s to image Alexa Fluor 488 streptavidin and 2 s to image rhodamine neutravidin.

Data analysis was conducted using ImageJ imaging software (available at http://rsbweb.nih.gov/ij/). Intensity measurements of microtubules loaded with streptavidin/neutravidin were made by subtracting the background (the mean value of the intensity counts of an 8 μm circular region near, but not on, the microtubule) from the mean value of the intensity counts of an 8 μm circular region centered on a microtubule. The intensity value represents the mean ± SEM of 24−30 individual intensity measurements. The kinetic model was fit using the nonlinear fitting tool of MATLAB (Mathworks, Natick, MA). Fit parameters E_0 and E_i are presented as the fitted parameter value ± the 95% confidence interval of the fitted value, based on the nonlinear fitting algorithm. E_0 was kept constant between the two fits for neutravidin adsorption.

ASSOCIATED CONTENT

Supporting Information

Data from kinetics experiments. Distribution of lysine groups on the tubulin heterodimer. Calculations of the expected interaction energy from electrostatic interactions, from steric hindrance, and from double-binding modeling. This material is available free of charge via the Internet at http://pubs.acs.org.

AUTHOR INFORMATION

Corresponding Author

*E-mail: hh2374@columbia.edu. Telephone: (212) 854-7749.

Author Contributions

†These authors contributed equally.

Notes

The authors declare no competing financial interest.

ACKNOWLEDGMENTS

S.H. thanks the Chinese Scholarship Council (CSC). A.T.L., Y.J.-S., and H.H. were supported by NSF grant DMR 1015486.

REFERENCES

(1) Yan, H.; Park, S. H.; Finkelstein, G.; Reif, J. H.; LaBean, T. H. DNA-templated self-assembly of protein arrays and highly conductive nanowires. *Science* **2003**, *301*, 1882−1884.

(2) Ringler, P.; Schulz, G. E. Self-assembly of proteins into designed networks. *Science* **2003**, *302*, 106−109.

(3) Keren, K.; Krueger, M.; Gilad, R.; Ben-Yoseph, G.; Sivan, U.; Braun, E. Sequence-specific molecular lithography on single DNA molecules. *Science* **2002**, *297*, 72−75.

(4) Niemeyer, C. M.; Adler, M.; Gao, S.; Chi, L. F. Supramolecular nanocircles consisting of streptavidin and DNA. *Angew. Chem., Int. Ed.* **2000**, *39*, 3055−3059.

(5) Lund, K.; Manzo, A. J.; Dabby, N.; Michelotti, N.; Johnson-Buck, A.; Nangreave, J.; Taylor, S.; Pei, R. J.; Stojanovic, M. N.; Walter, N. G.; Winfree, E.; Yan, H. Molecular robots guided by prescriptive landscapes. *Nature* **2010**, *465*, 206−210.

(6) Hess, H.; Clemmens, J.; Brunner, C.; Doot, R.; Luna, S.; Ernst, K.-H.; Vogel, V. Molecular self-assembly of "nanowires" and "nanospools" using active transport. *Nano Lett.* **2005**, *5*, 629−633.

(7) Bachand, M.; Trent, A. M.; Bunker, B. C.; Bachand, G. D. Physical factors affecting kinesin-based transport of synthetic nanoparticle cargo. *J. Nanosci. Nanotechnol.* **2005**, *5*, 718−722.

(8) Liu, H. Q.; Spoerke, E. D.; Bachand, M.; Koch, S. J.; Bunker, B. C.; Bachand, G. D. Biomolecular motor-powered self-assembly of dissipative nanocomposite rings. *Adv. Mater.* **2008**, *20*, 4476−4481.

(9) Kawamura, R.; Kakugo, A.; Osada, Y.; Gong, J. P. Microtubule bundle formation driven by ATP: the effect of concentrations of kinesin, streptavidin and microtubules. *Nanotechnology* **2010**, *21*, 145603.

(10) Choi, D. S.; Byun, K. E.; Hong, S. Dual transport systems based on hybrid nanostructures of microtubules and actin filaments. *Small* **2011**, *7*, 1755−1760.

(11) Tarhan, M. C.; Yokokawa, R.; Bottier, C.; Collard, D.; Fujita, H. A nano-needle/microtubule composite gliding on a kinesin-coated surface for target molecule transport. *Lab Chip* **2010**, *10*, 86−91.

(12) Fischer, T.; Agarwal, A.; Hess, H. A smart dust biosensor powered by kinesin motors. *Nat. Nanotechnol.* **2009**, *4*, 162−166.

(13) Ramachandran, S.; Ernst, K.-H.; Bachand, George D.; Vogel, V.; Hess, H. Selective loading of kinesin-powered molecular shuttles with protein cargo and its application to biosensing. *Small* **2006**, *2*, 330−334.

(14) Schmidt, C.; Vogel, V. Molecular shuttles powered by motor proteins: loading and unloading stations for nanocargo integrated into one device. *Lab Chip* **2010**, *10*, 2195−2198.

(15) Korten, T.; Diez, S. Setting up roadblocks for kinesin-1: mechanism for the selective speed control of cargo carrying microtubules. *Lab Chip* **2008**, *8*, 1441−1447.
(16) Langmuir, I. The constitution and fundamental properties of solids and liquids. Part I. Solids. *J. Am. Chem. Soc.* **1916**, *38*, 2221−2295.
(17) Fowler, R. H.; Guggenheim, E. A. *Statistical Thermodynamics*; University Press: Cambridge, U.K., 1960.
(18) Hamdaoui, O.; Naffrechoux, E. Modeling of adsorption isotherms of phenol and chlorophenols onto granular activated carbon. Part I. Two-parameter models and equations allowing determination of thermodynamic parameters. *J. Hazard. Mater.* **2007**, *147*, 381−394.
(19) Temkin, M.; Pyzhev, V. Kinetics of ammonia synthesis on promoted iron catalysts. *Acta Physicochim. URSS* **1940**, *12*, 327−356.
(20) Langmuir, I. The evaporation, condensation and reflection of molecules and the mechanism of adsorption. *Phys. Rev.* **1916**, *8*, 149−176.
(21) Feder, J. Random sequential adsorption. *J. Theor. Biol.* **1980**, *87*, 237−254.
(22) Ray, S.; Meyhöfer, E.; Milligan, R. A.; Howard, J. Kinesin follows the microtubule's protofilament axis. *J. Cell Biol.* **1993**, *121*, 1083−1093.
(23) Agarwal, A.; Katira, P.; Hess, H. Millisecond curing time of a molecular adhesive causes velocity-dependent cargo-loading of molecular shuttles. *Nano Lett.* **2009**, *9*, 1170−1175.
(24) Haugland, R. P.; You, W. W. Coupling of antibodies with biotin. *Methods Mol. Biol.* **1998**, *80*, 173−183.
(25) Green, N. M. Avidin and streptavidin. *Methods Enzymol.* **1990**, *184*, 51−67.
(26) Sivasankar, S.; Subramaniam, S.; Leckband, D. Direct molecular level measurements of the electrostatic properties of a protein surface. *Proc. Natl. Acad. Sci. U.S.A.* **1998**, *95*, 12961−12966.
(27) Lin, C. T.; Kao, M. T.; Kurabayashi, K.; Meyhofer, E. Self-contained biomolecular motor-driven protein sorting and concentrating in an ultrasensitive microfluidic chip. *Nano Lett.* **2008**, *8*, 1041−1046.
(28) Kerssemakers, J.; Howard, J.; Hess, H.; Diez, S. The distance that kinesin-1 holds its cargo from the microtubule surface measured by fluorescence interference contrast microscopy. *Proc. Natl. Acad. Sci. U.S.A.* **2006**, *103*, 15812−15817.
(29) Stamm, C.; Lukosz, W. Integrated optical difference interferometer as biochemical sensor. *Sens. Actuators, B* **1994**, *18*, 183−187.
(30) Chilkoti, A.; Stayton, P. S. Molecular origins of the slow streptavidin-biotin dissociation kinetics. *J. Am. Chem. Soc.* **1995**, *117*, 10622−10628.
(31) Kolasinski, K. W. *Surface Science: Foundations of Catalysis and Nanoscience*. Wiley: Chichester, England, 2008.
(32) Jung, L. S.; Nelson, K. E.; Stayton, P. S.; Campbell, C. T. Binding and dissociation kinetics of wild-type and mutant streptavidins on mixed biotin-containing alkylthiolate monolayers. *Langmuir* **2000**, *16*, 9421−9432.
(33) Jung, L. S.; Campbell, C. T. Sticking probabilities in adsorption of alkanethiols from liquid ethanol solution onto gold. *J. Phys. Chem. B* **2000**, *104*, 11168−11178.
(34) *Laboratory Studies of Heterogeneous Catalytic Processes*; Christoffel, E. G., Paál, Z., Eds.; Studies in Surface Science and Catalysis; Elsevier: Amsterdam, 1989; Vol. *42*, Chapter 2, pp 7−45.
(35) Moy, V. T.; Florin, E.-L.; Gaub, H. E. Intermolecular forces and energies between ligands and receptors. *Science* **1994**, *266*, 257−259.
(36) Adamczyk, Z. Kinetics of diffusion-controlled adsorption of colloid particles and proteins. *J. Colloid Interface Sci.* **2000**, *229*, 477−489.
(37) Hucknall, A.; Kim, D.-H.; Rangarajan, S.; Hill, R. T.; Reichert, W. M.; Chilkoti, A. Simple fabrication of antibody microarrays on nonfouling polymer brushes with femtomolar sensitivity for protein analytes in serum and blood. *Adv. Mater.* **2009**, *21*, 1968−1971.
(38) Xu, X.; Georganopoulou, D. G.; Hill, H. D.; Mirkin, C. A. Homogeneous detection of nucleic acids based upon the light scattering properties of silver-coated nanoparticle probes. *Anal. Chem.* **2007**, *79*, 6650−6654.
(39) Vilfan, A.; Frey, E.; Schwabl, F.; Thormahlen, M.; Song, Y. H.; Mandelkow, E. Dynamics and cooperativity of microtubule decoration by the motor protein kinesin. *J. Mol. Biol.* **2001**, *312*, 1011−1026.
(40) Roos, W. H.; Campas, O.; Montel, F.; Woehlke, G.; Spatz, J. P.; Bassereau, P.; Cappello, G. Dynamic kinesin-1 clustering on microtubules due to mutually attractive interactions. *Phys. Biol.* **2008**, *5*, 046004.
(41) Zhao, S.; Walker, D. S.; Reichert, W. M. Cooperativity in the binding of avidin to biotin-lipid-doped Langmuir-Blodgett films. *Langmuir* **1993**, *9*, 3166−3173.
(42) Zhao, S.; Reichert, W. M. Analysis of protein binding to receptor-doped lipid monolayers by Monte Carlo simulation. *Biophys. J.* **1994**, *66*, 305−309.
(43) Coy, D. L.; Hancock, W. O.; Wagenbach, M.; Howard, J. Kinesin's tail domain is an inhibitory regulator of the motor domain. *Nat. Cell Biol.* **1999**, *1*, 288−292.